Final Report

Monitoring of Hydrologic Effects of Salt Cedar Control in the Upper Brazos River Basin, Texas

August 31, 2019

Brad D. Wolaver[1], Azadeh Gholoubi[1], Todd G. Caldwell[2], Tara Bongiovanni[1], Jon Paul Pierre[1]

[1]Bureau of Economic Geology, Jackson School of Geosciences, The University of Texas at Austin, Austin, Texas 78758, USA; Corresponding author: brad.wolaver@beg.utexas.edu.

[2]Bureau of Economic Geology, Jackson School of Geosciences, The University of Texas at Austin, Austin, Texas 78758, USA; Currently: U.S. Geological Service, Nevada Water Science Center, 2730 N Deer Run Rd, Carson City, Nevada 89701

Submitted to:

Texas Parks and Wildlife Department, Austin, TX

TPWD Contract No. 505176

Table of Contents

List of Figures

1 Executive Summary

Invasive saltcedar (*Tamarix* spp.) is found throughout the upper Brazos River (UB) basin in the Southwestern Tablelands ecoregion of West Texas. The armoring of stream banks and sandbars by saltcedar may reduce stream width, deepen stream channels, and increase current velocities. Saltcedar has also been suspected as a relatively high user of alluvial groundwater and soil moisture. Therefore, saltcedar control has been considered as a potential strategy for conserving water, increasing streamflow, and restoring natural channel hydraulics and riparian habitat. Thus, the goal of this study is to monitor soil moisture in the unsaturated zone, groundwater level and conductivity in UB alluvial aquifers, and precipitation to characterize UB hydrology and evaluate the efficacy of herbicide treatment on saltcedar stands to change water use. Specifically, this study focuses on surface and groundwater exchange in shallow alluvial aquifers, addressing questions such as: How does saltcedar abatement affect baseflow? When does the river gain water from or lose water to the aquifer, and how does this process vary depending on season and stream stage? We evaluated river baseflow, storm flow, and total flow changes at upstream USGS gages to assess subbasin-scale streamflow gain and loss. We also determined soil and alluvial aquifer water storage, groundwater flux, hydraulic gradient magnitude, and groundwater flow direction changes. We estimated evapotranspiration (ET) during the study time by measuring diurnal soil-water content changes from soil surface to a 50-cm depth, as well as by measuring diurnal groundwater table fluctuations using a method developed by White (1932). Ultimately, this study improves our understanding of soil water and groundwater fluxes at representative UB saltcedar stands.

From 2016 to 2019, Texas Parks and Wildlife Department (TPWD) treated saltcedar along the UB using aerial application of imazapyr herbicide by helicopter. Beginning in late September

2016, The University of Texas at Austin Bureau of Economic Geology (UT-BEG) established six monitoring sites along the Double Mountain Forks Brazos River (DMF), Salt Fork Brazos River (SF), and UB to quantify potential hydrological effects of saltcedar abatement. Each of the six sites consists of one precipitation gage and three monitoring wells with co-located soil moisture sensors located on incrementally higher alluvial terraces with riparian saltcedar. Monitoring equipment was installed at sites DMF1 and DMF2 on Sept. 21–22, 2016 and at DMF3, SF1, SF2, UB1 on June5–9, 2017. The last data download under this contract occurred May 28, 2019. As data collected during the first month were noisy, the main period of hydrologic data analysis for this study is July 1, 2017 to May 28, 2019.

For most of our study locations, results of ET estimation from groundwater fluctuations did not show appreciable changes following saltcedar abatement—with some important caveats. For example, some monitoring sites were not directly treated with herbicide and treatment varied spatially and temporally during each of the three years that treatment occurred. In addition, the study presents a relatively short monitoring period following treatment. Given these study limitations, our evaluation of alluvial aquifer hydraulic gradients showed that groundwaters flows relatively parallel to the stream during the study period at most of our UB study locations. Thus, during the majority of the monitoring period, hydraulic gradients did not suggest appreciable groundwater inflows to the stream from surrounding aquifers. During floods, rapid increases in alluvial aquifer groundwater levels and speedy declines (on the order of weeks to a few months) suggests that (1) alluvial aquifer recharge from high streamflows is minimal, (2) even under high-flow conditions the stream is not losing significant water volume to the alluvial aquifer, and (3) multi-year leakage of bank storage to streams—as observed on other western United States

river systems—does not appreciably support streamflow during summers and droughts. These points are supported by the low correlation between stream stage and alluvial storage during high streamflow at most monitoring sites. Treatment of additional hectares is ongoing in 2019 and is expected to continue through and past 2021. The results of proposed continued hydrologic monitoring will refine estimates of ET and alluvial aquifer dynamics to better understand the effects of saltcedar treatment on soil moisture, alluvial aquifer groundwater levels, and streamflow.

This report also serves as an update of fiscal year (FY) 2019 work. All six established sites (18 data acquisition stations total) were maintained and continue to upload data to the Texas Soil Moisture Observation Network (TxSON, 2019). Data presentation on the website was changed somewhat from using Campbell Scientific LoggerNet to MatLAB scripts, which improved the filtering out of potentially erroneous data. A few groundwater monitoring sensors were replaced, including DMF2_L in January 2019 and again in April 2019 as well as DMF3_M (due to failure of the sensors). Well development using a portable submersible pump to remove sediment which accumulated in the bottom of the wells during installation was completed by Sunbelt Industrial Services (Fort Worth, TX) in April 2019 and successfully produced low-turbidity, clear water at most sites. To improve our characterization of groundwater movement through the alluvial aquifer, we conducted slug test in monitoring wells to estimate hydraulic conductivity. Slug tests were conducted in FY 2018, finalized during FY 2019, and presented in this report. Alluvial aquifer sediment particle size analysis was also completed in FY 2019 and included here to provide insight into expected behavior of soil moisture in the unsaturated root zone. The remainder of this report is in the format of a draft manuscript we prepared in FY 2019 and, after refining the content, plan to ultimately submit to a peer-reviewed journal.

2 Introduction

Invasive saltcedar (*Tamarix* spp.) has altered riparian plant communities along regulated rivers throughout the western United States, changing channel morphology and replacing transpiration by native riparian vegetation with potentially deeper-rooted saltcedar (McDonald et al., 2015). The historical belief that saltcedar uses more water than native vegetation, brought into question by a number of studies, has led to substantial eradication efforts. For example, saltcedar transpiration on a portion of the UB was estimated by an early study to use 44,000 acre-ft per year (Busby and Schuster, 1973). However, recent studies have found that improved water yields following watershed-scale saltcedar control efforts are seldom quantifiable (Doody et al., 2011; Wilcox, 2002; Wilcox et al., 2006). One such small-scale control program on the Pecos River in Texas produced negligible water gains because the old-stand age saltcedar used minimal water compared to the relatively high streamflows in the study reach (McDonald et al., 2013; McDonald et al., 2015). It is important to note that compared to the UB study area of this study, the Pecos River location studied by McDonald et al. (2013, 2015) (1) investigated only a 3 km reach, (2) had saltcedar only in a narrow band of ~50 m on either side of the river, and (3) was a losing streamflow to surrounding aquifers. Thus, this study assesses a much larger area, with wider stands of saltcedar (>200 m in some places), and primarily gaining stream conditions (Baldys and Schalla, 2011).

Saltcedar also affects stream geomorphology by colonizing stream floodplains and terraces, reducing the ability of the stream to meander, causing sediment accumulation, and narrowing the stream channel (Dean et al., 2011; Nagler et al., 2009). Armoring of banks with saltcedar can change a wide, shallow and braided, low-velocity stream to a narrower, deeper, faster-moving flow, with potential adverse impacts to native fish. In the main-stem Brazos River

between Possum Kingdom Lake and the confluence of the Double Mountain Fork Brazos River (DMF), which is up to ~200 km downstream of this study area (i.e., higher stream discharge, wider channel, etc., than further upstream), surveys of woody phreatophyte vegetation in the floodplain revealed an increase from 39 percent in 1969 to 57 percent by 1979 (Blackburn et al., 1982). Saltcedar-dominated areas where the floodplain was narrow and the stream channel was straight provided optimum water-table conditions for their growth and regeneration (Busby and Schuster, 1973). Saltcedar invasion also caused up to 3 m of sediment accumulation in some places and reduced the Brazos River width by ~90 m, reduced sediment input to Possum Kingdom, and resulted in higher flood stages. Thus, an additional potential benefit of saltcedar control, includes restoration of river geomorphology when subsequent floods remove dead saltcedar and mobilize sediment (Perignon et al., 2013; Vincent et al., 2009) and recovery of native plant communities and wildlife habitat in riparian and floodplain areas.

The goals of this study are to gain a better understanding of surface water and groundwater interaction by monitoring post-abatement effects on local and regional hydrology in the UB basin and to characterize ET at our study sites along the UB. We instrumented six sites with three monitoring locations located in treated (at different times) riparian areas and monitored soil moisture and alluvial aquifer groundwater. We compared the hydraulic head differences with direct, river-based subsurface discharge measurements and assessed the relative importance of alluvial aquifer-stream interactions.

By evaluating continuous monitoring data from groundwater wells, soil moisture, river stage, and aquifer storage, this study addresses these questions:

- When is the river gaining or losing, and does this vary by season and stage?
- What controls groundwater flux, and how does alluvial storage respond to changes in river stage?
- What is the linkage between saltcedar abatement and streamflow?
- How does the ET rate from groundwater and soil change during the study period and before/after saltcedar abatement?

We apply this approach to the UB; however, these methods may be used to assess stream-alluvial aquifer-riparian vegetation interactions in similar semi-arid and arid streams.

3 Material and methods

3.1 Site description

The focus of this research is the upper Brazos River (UB) and its major tributaries, the Salt Fork Brazos River (SF) and Double Mountain Forks Brazos River (DMF), located upstream of Possum Kingdom Lake. The UB is characterized by shallow, sandy, braided stream channels (Mayes et al., 2019). The SF is fed by numerous Permian brine springs and at times leads to salinities >90,000 mg/L total dissolved solids (Baker et al., 1964; Brune, 2002) and clear waters. The White River, a tributary of the Salt Fork, was once fed by the fresher Ogallala Aquifer at the rate of 49,210 m^3/day (~20 ft^3/s) (Evermann and Kendall, 1894) and was impounded in 1963 with the construction of the White River Reservoir. Leakage from the dam forms a small trickle, and groundwater pumping for irrigation has dried up nearly all springs fed by the Ogallala in the Salt

Fork watershed (Brune, 2002). Lake Alan Henry, impounded January 1994 to provide water supply to the City of Lubbock, is located on the South Fork DMF before its confluence with the North Fork DMF. Portions of the DMF are also underlain by the Ogallala (Brune, 2002). Study sites (Figure 1) were selected based in collaboration with Texas Parks and Wildlife Department (TPWD) to be located in sites with variable saltcedar density along the UB (as measured during helicopter surveys).

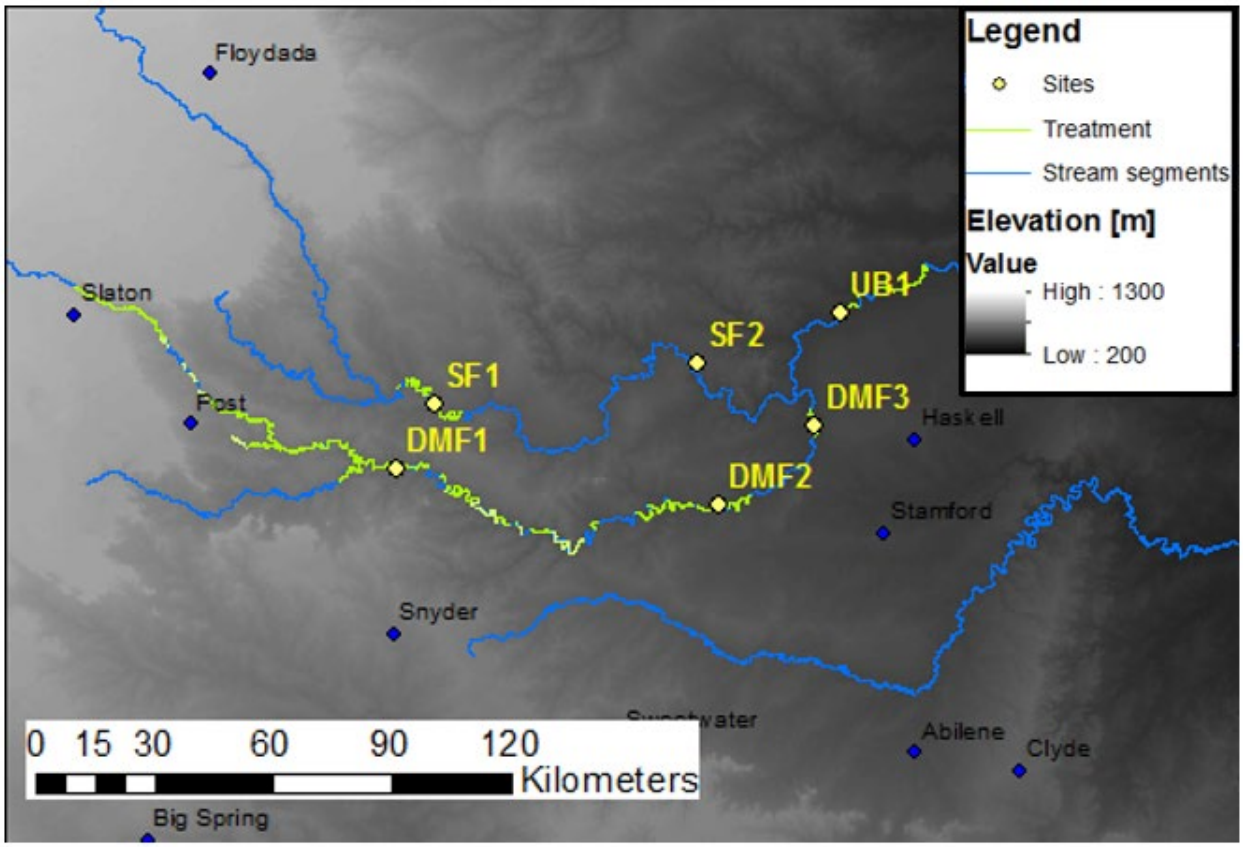

Figure 1. Site map of monitoring locations on the Double Mountain Forks, Salt Fork, and Upper Brazos Rivers.

Yellow dots and labels are monitoring locations: DMF: Double Mountain Forks Brazos River, SF: Salt Fork Brazos River, UB: upper Brazos River. Herbicide treatment locations for 2016–2018 are shown as green (McGarrity, 2019).

Soils throughout the UB are derived from Permian calcareous and gypsiferous rocks and mudstones of the Clairemont–Yahola–Lincoln soil association. Deposits of the upper and middle terraces are generally mapped as Clairemont silt loam, a calcareous silty alluvium derived from siltstones or Lincoln loamy fine sands. The lowest terrace is generically designated riverwash—a loamy fine sand. During sensor installation, nearly all soils (to 1-m depth) were fine-grained sands with little noticeable structure and only modest accumulations of organic material in the A horizon. Roots were sparsely noted, as well. Boreholes for groundwater monitoring well installation were drilled into river alluvium until refusal occurred at the depth of a regionally extensive greenish-gray clay. Depth to water was obtained using an electric wireline sounder ("e-line") to measure the distance from the well casing top (which serves as our datum recorded by the Global Navigation Satellite System [GNSS]) to the water table. The static water elevation represents the absolute groundwater elevation after installation corrected for datum elevation and sensor depth. Monitoring sites were selected based on the following criteria:

- Geographic distribution within a saltcedar abatement area from the headwaters of the DMF and SF to its confluence at the UB;
- Providing a range of low to high saltcedar density;
- Geomorphology of available stream reach;
- Landowner permission and accessibility for equipment; and
- Location close to bridges where either the USGS had river-stage recorders or where UT-BEG could install gages.

3.2 Field installation

Beginning in late September 2016, we established six monitoring sites along the DMF, SF, and UB. Each site consists of three nested monitoring wells. Each site was chosen to represent lesser versus greater degree of saltcedar infestation sites on each fork. Groundwater and soil moisture monitoring equipment was installed at sites DMF1 and DMF2 on Sept. 21–22, 2016 and at DMF3, SF1, SF2, and UB1 on June 5–9, 2017. The last data download under this contract occurred May 28, 2019. In order to avoid inclusion of somewhat noisy data collected during the first month after installation, the analysis period for this study is July 1, 2017 to May 28, 2019. Each well location was chosen for a range of geomorphic positions above the stream channel. The first was on the lowest ("L"; e.g., DMF_L) alluvial terrace, approximately 1.5–3 m above baseflow levels; the highest ("U") well was situated above the riparian area; and the last well ("M") was placed on a terrace in between. The combination of the three wells enabled the determination of local groundwater gradient between water table and the river.

Well installation was done by Sunbelt Industrial Services (Fort Worth, TX) using a Geoprobe equipped with a 15.24-cm (6-inch) outer-diameter hollow-stem auger. A 5.08-cm (2-inch) inner-diameter schedule 40 PVC casing and screen was installed to a total depth ranging from 4.5–15 m below ground surface (bgs). Our goal was to have the screen interval for each of the three wells lie within the same alluvial aquifer (perched on a gray, gravelly clay, which also formed the bottom of the stream channel at most sites). Thus, lower terrace wells are shallower than the higher wells, but all are essentially in hydraulic communication with each other. Well elevation was determined using Trimble TRM59800 GNSS antennas with accompanying NetR9 receivers. To accurately determine elevation and position, two antennas were used. Static points

were set and continuously recorded while a mobile rover concurrently collected measurements at specific locations. The known point for our eastern locations was the airport in Haskell, Texas. For wells DMF1 and SF1, the Continuously Operating Reference Stations (CORS) of the National Geodetic Survey Office was used for the static point. Using GNSS data collected from a known reference point allows for error correction of the rover data. We did corrections using NovAtel's GrafNav software via differential post-processing to obtain a high degree of accuracy. The lateral error in both latitude and longitude was theoretically 2 cm; the vertical was 4 cm. Relative elevations of each well were determined by traditional surveys using a stadia rod and transit.

Each well is equipped with a Decagon Devices conductivity/depth/temperature (CDT) sensor to continuously monitor groundwater level and temperature. Groundwater level was used to assess the extent to which floods may recharge the alluvial aquifer and potentially provide subsequent groundwater flows to the stream.

Groundwater elevations indicate the direction of water flux based on the hydraulic head between each well. To obtain this groundwater elevation, we subtracted the length of the sensor cable from the elevation derived for GNSS at a specific mark (i.e., elevation datum) on the well casing. The pressure head read by the sensor (in mm of groundwater) is added to get the absolute elevation time series. The sensors were vented to the atmosphere, so no further corrections were required to account for changes in barometric pressure.

Five soil moisture sensors (Campbell Scientific, CS655), co-located at monitoring wells, were installed at 5-, 10-, 20-, 50-, and 100-cm depths to measure soil saturation. The CS655 sensors measure volumetric water content using time-domain reflectometry. The sensors were installed horizontally into a hand-dug soil pit 3–4 m away from each well. Sensor wires were buried at

20 cm (~8 inches), then routed through the concrete well pad in a PVC conduit and connected to a data acquisition station, which powers all sensors and collects and stores data.

At DMF 1 and DMF2, sensors were connected to a data logger (Campbell Scientific, CR200) with integrated solar power and cellular communications (i.e., three cell modems per site). At DMF3, SF1, SF2, and UB1, a datalogger with radio communication (Campbell Scientific, CR300) was used so only one cell modem at the upper terrace site was needed. River stage was recorded hourly (In-Situ Rugged TROLL 100). Barometric pressure was recorded at DMF1, DMF2, and UB1. The pressure transducers were corrected using the barometric pressure from the closest location to get relative stage. The elevation survey provided the difference in elevation between the lower well and the piezometer which housed the Rugged TROLL. A precipitation gauge (Texas Electronics TE525) was also installed at each site (Figure 2).

Figure 2. Representative monitoring site, including solar panel, rain gage, and data-logger. Site shown is enclosure at DMF1 middle terrace well.

3.3 Herbicide application at saltcedar stands

Saltcedar herbicide treatment was accomplished by means of aerial herbicide application of imazapyr (EPA Registration #81927-23; 52.6% active ingredient; one quart per acre) and a nonionic surfactant (six ounces per acre), with focus on highly infested DMF sites. Treatment of study sites occurred 2016–2019 at specified locations of our study sites (Figure 3, Figure 4) (McGarrity, 2019). The site DMF1 was treated during 2016. In 2017, ~50 km upstream DMF1 and ~50 km upstream DMF2 was treated in 2017. Four sites (SF1, DMF2, DMF3, and UB1) were treated during 2018. The site at SF2 was the only site that had not yet received treatments as of 2018.

3.4 Data acquisition system

Groundwater and soil sensors are queried every 5 min and averaged hourly until June 2018 when 30-minute averaging began. Means are telemetered over the cellular network and archived at UT-BEG. The data are also posted in real time to the Texas Soil Observation Network (TxSON, 2019) website. Data visualization was done using the Campbell Scientific data collection Real-Time Monitoring and Control Software toolbox (LoggerNet Version 4.4.2). The location of the wells forms a triangle (Figure 5) across the treated riparian zone so that the magnitude and direction of hydraulic gradient can be calculated at each location using the three-point problem method (Heath, 1998). For this method, groundwater elevation data and location on a map were used for each well.

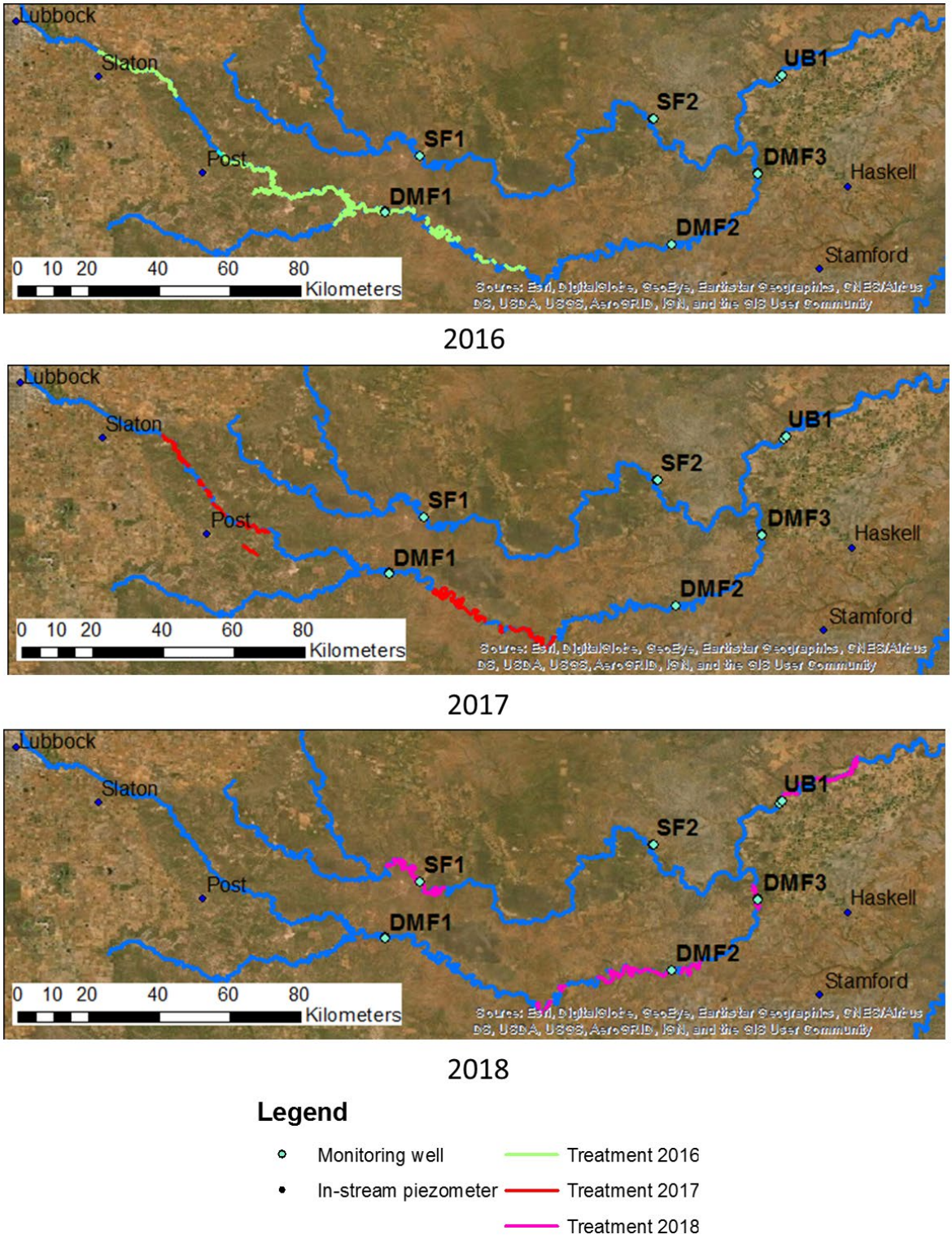

Figure 3. Locations of aerial application of imazapyr for entire study area.

Source: McGarrity (2019)

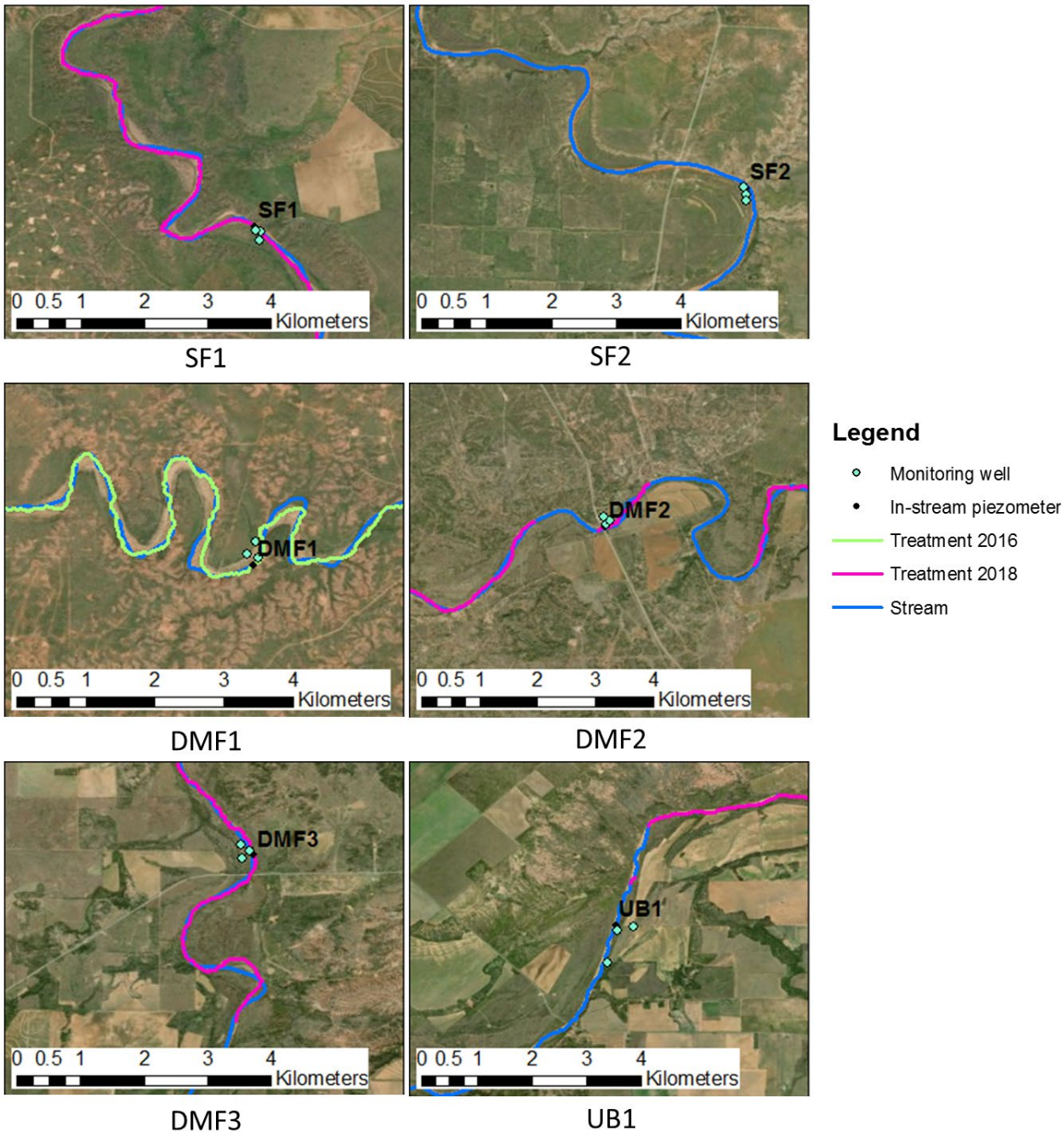

Figure 4. Locations of aerial application of imazapyr for each monitoring location.

Source: McGarrity (2019)

Figure 5. Representative monitoring well configuration (DMF1).

Typical configuration consists of an upper alluvial terrace well (DMF1_U), a midpoint location (DMF1_M), and a lower position adjacent to the stream (DMF1_L).

3.5 Sediment sampling and characterization

Soil and sediments samples were collected during the installation of soil sensors and groundwater monitoring wells. Soil samples were collected from 0-10, 20, 50 and 100 cm depth. Sediment samples were collected from cuttings approximately every 1.5 m. Particle size distribution (PSD) was measured using a combination of dry-sieve and Bouyoucous laser diffraction methods (LDM). Soil samples were air-dried, gently crushed, and dry-sieved at 2000-µm mesh size. Carbonates and iron oxides were not removed because doing so is optional using the standard method. A Mastersizer 3000 (Malvern Instruments, UK) laser diffractometer, which measures within a size

range of 0.01–3500 µm (Malvern, 2013), was used for LDM analysis. The mass of dry soil samples placed into the dispersion unit was in the range of 0.5–1.0 g, depending on the "obscuration" of the soil suspension after dispersion. In this context, obscuration is a measure of the amount of light scattered by the soil particles and correlates with the concentration of measured material present in the laser diffractometer. Obscuration values should be between 1 and 10 percent for the dry dispersion unit (Malvern, 2013). The PSD was determined on two or three replicates (measurement of distinct subsamples) using LDM. If the shapes of the PSD curves of two repetitions were largely dissimilar, a third measurement was made.

3.6 Aquifer characterization

Slug tests (Bouwer and Rice, 1976) were conducted in each monitoring well to estimate the saturated hydraulic conductivity (K) of the screened layer. Transmissivity (T) is the rate of flow under a unit hydraulic gradient through a unit width of an aquifer of given saturated thickness (b) is estimated using equation 1:

$$T = Kb \qquad [1]$$

3.7 Soil-water storage

Soil-water storage from soil surface to 50-cm depth is calculated using the sum of the results of multiplying soil daily mean values of volumetric water content (VWC) by the related distance of each VWC.

3.8 Soil evapotranspiration and root water uptake

A method based on the diurnal cycle of water uptake by vegetation, which peaks during daylight hours, was used to estimate ET (Gribovszki et al., 2010; Guderle and Hildebrandt, 2015; Hupet et

al., 2002; Naranjo et al., 2011; White, 1932). The single-step, multilayer (SSML) water-balance method used to calculate water extraction from soil by plant roots and soil evaporation (sink term) is based on two observation times (single-step) and several measurement depths (multilayer). This method requires a volumetric soil-water content time series and rainfall measurements of selected dry periods (24 hours after a precipitation event). The water balance during dry periods of each layer is determined (equation 3); to calculate uptake in individual layers. Using this method, the change in soil-water content is assumed to be caused only by root-water uptake, so vertical soil-water fluxes are neglected (Clothier and Green, 1994; Guderle and Hildebrandt, 2015; Hupet et al., 2002):

$$S_{ssml} = d_{z,i} \frac{\Delta\theta_i}{\Delta t} \qquad [2]$$

where S_{ssml} is the estimated sink term in soil layer i, $\Delta\theta_i$ is soil-water content change in i soil layer over the single time step (Δt), z is soil depth, and $d_{z,i}$ is soil layer i thicknesses. Actual evapotranspiration (ET) is calculated by summing up $S_{ssml\,,i}$ over all depths (equation 3):

$$ET = \sum_{i=1}^{n} S_{ssml_i} \qquad [3]$$

3.9 Groundwater evapotranspiration

In addition to assessing diurnal soil moisture fluctuations, diurnal groundwater fluctuations can also be used to infer evapotranspiration (i.e., daily water consumption) from phreatophytic vegetation (Fahle and Dietrich, 2014). Estimating groundwater evapotranspiration (ET_g) was initially introduced by White (1932) and more recently improved by Loheide (2008) and Gribovszki et al. (2010). In arid and semiarid environments, low precipitation and high potential ET generally creates a dry, shallow soil layer and a deep water table. However, in the case of the

deep-rooting *Tamarix*, the roots of the plants can access soil moisture from 4 m deep (Wang et al., 2019). Therefore, groundwater serves as a reliable water source for phreatophytic vegetation, such as *Tamarix.* Evapotranspiration from alluvial aquifer groundwater is calculated using the approach of White (1932):

$$ET_g = S_y(\frac{\Delta s}{t} + R) \qquad [4]$$

where ET_g is the rate of groundwater consumed by evapotranspiration averaged over a 24-hr day (mm), *Sy* is the specific yield (dimensionless), *Δs* is the daily change in storage that is calculated as the net rise or fall of the water table (mm) from 00:00 (i.e., 12 a.m.) on the day being analyzed to 00:00 on the preceding day. Net inflow (*R*, recovery) rate (mm/day) is determined from the hourly rate of change in water-table elevation during the hours from 00:00 to 04:00 (i.e., 4 a.m.), when transpiration is assumed to be negligible. This method is based on four assumptions (Loheide et al., 2005): (1) diurnal water-table fluctuations are a function of plant water use; (2) groundwater consumption by plants is negligible between midnight and 4 a.m. when water flows from areas of higher hydraulic head to areas of lower hydraulic head to replace water extracted during the day; (3) the rate of flow is constant into the near-well region throughout the entire day; and (4) a representative value of specific yield can be computed. Loheide et al. (2005) introduced S_y^*, a novel approach to assess readily available specific yield. The important difference between the classically defined specific yield and that of Loheide et al. (2005) is that the latter is associated with short time scales and a shallow water table (Meyboom, 1967; Nachabe, 2002). To characterize specific yield, we conducted a sediment texture analysis for each site and then related texture to specific yield using a database in Loheide et al. (2005).

To satisfy the assumption that diurnal water-table functions are only a function of plant uptake, data values associated with precipitation events were removed for the purpose of this analysis. This removal was necessary because increased groundwater levels caused by precipitation events significantly influence the computed recovery rate and produce estimates of ET_g that are negative and/or strongly skewed (Runyan and Welty, 2010).

3.10 Alluvial water storage

Water storage in the alluvial aquifer (A) was calculated at each monitoring well using saturated porosity (P, soil saturated water content from 100-cm soil moisture sensor) and the thickness of saturated groundwater (t) calculated at each well as groundwater elevation measured at each time step minus the minimum groundwater elevation measured during the study period, using equation 5:

$$A = Pt \qquad [5]$$

3.11 Groundwater hydraulic gradients

Hydraulic gradient is the driving force of groundwater moving in the direction of maximum decrease of total head (Mazor and Nativ, 1992), determined using the three-point method (Heath, 1998). In this method, the direction of groundwater movement and hydraulic gradient, determined by information from three wells (water-level elevations and well location) at each of six monitoring sites. A Python programming code is used to compute the distance between wells, and hydraulic-gradient magnitude and direction using the three-point method (e.g., Van Rossum and Drake, 2011).

3.12 Groundwater flux

Darcy's law is used to calculate groundwater flux,J_w, (mm/day) through a unit area of alluvial aquifer using the average hydraulic conductivity of the three wells at each site, K_s, (m/day) and hydraulic gradient, i, (mm/m):

$$J_w = -K_s . i \qquad [6]$$

Python scripting is used for all analyses and output visualization.

4 Results and discussion

4.1 Sediment sampling and characterization

Only DMF1_U, DMF2_U, and SF1_U had noticeable soil formation, including hard pans at depth, which were potentially related to prior agricultural practices. In general, sediment of the alluvial aquifer was mostly sandy (fine to medium fine) with low water-holding capacity and little horizonation or structure. Such soils (or alluvium) would favor deeply rooted vegetation where infiltrating water with lower salinity would migrate quickly to depth and not be lost to evaporation. Static groundwater level immediately following well installation on each site had a mean of 1.08 m and a median of 0.35 m, indicating that most sites have a relatively flat water table. The minimum difference was 0.05 m at DMF3; the maximum was 4.16 m at SF1.

The results of soil-particle size distribution, aquifer transmissivity, screen interval, depths of soil and groundwater sensors, and groundwater elevation are presented on Figure 6. Alluvial aquifer particle-size distribution varied from clay to gravel. DMF1_L had the greatest percentage of coarse-grained materials in any well, with more than 85 percent gravel (greater than 2 mm) and less

than two percent fine-grained material (less than 0.25 mm). Overall, the alluvial aquifer was primarily comprised of fine- to medium-grained sands, accounting for as much as 80 percent of the material.

4.2 Aquifer characterization

Results of alluvial aquifer slug tests revealed transmissivity values that varied within two orders of magnitude. When considering the saturated alluvial aquifer thickness (Figure 6), resulting hydraulic conductivity values are approximately 10^{-6} to 10^{-4} m/s, which is consistent with silty sand to gravel (Freeze and Cherry, 1979) typically found in alluvial aquifers such as those in this study.

4.3 Soil-water storage

Figure 7 shows July 2017–June 2019 changes in soil water storage to 50 cm depth. At DMF1, DMF3, and SF1, soil-water content at lower terrace wells was higher than at the two other wells, which is consistent with capillary rise from a shallow water table ~1 m below land surface (Figure 6) and the proximity of the lower terrace well to the stream (i.e., source of soil moisture). Soil-water storage was mainly controlled by capillary effect and varied with groundwater level or storage. The lower three wells had no discernable diurnal fluctuation in soil-water content. Increases in stream stage at lower terrace wells during episodic floods caused water to enter the alluvial aquifer, raise groundwater levels, and increase soil-water storage starting around September 2018. At this time, the soil became saturated with a soil-water content of approximately 0.5 cm^3cm^{-3}. Additionally, increases in soil-water content at all other wells was primarily caused by persistent precipitation starting around September 2018. Minimum soil-water storage during

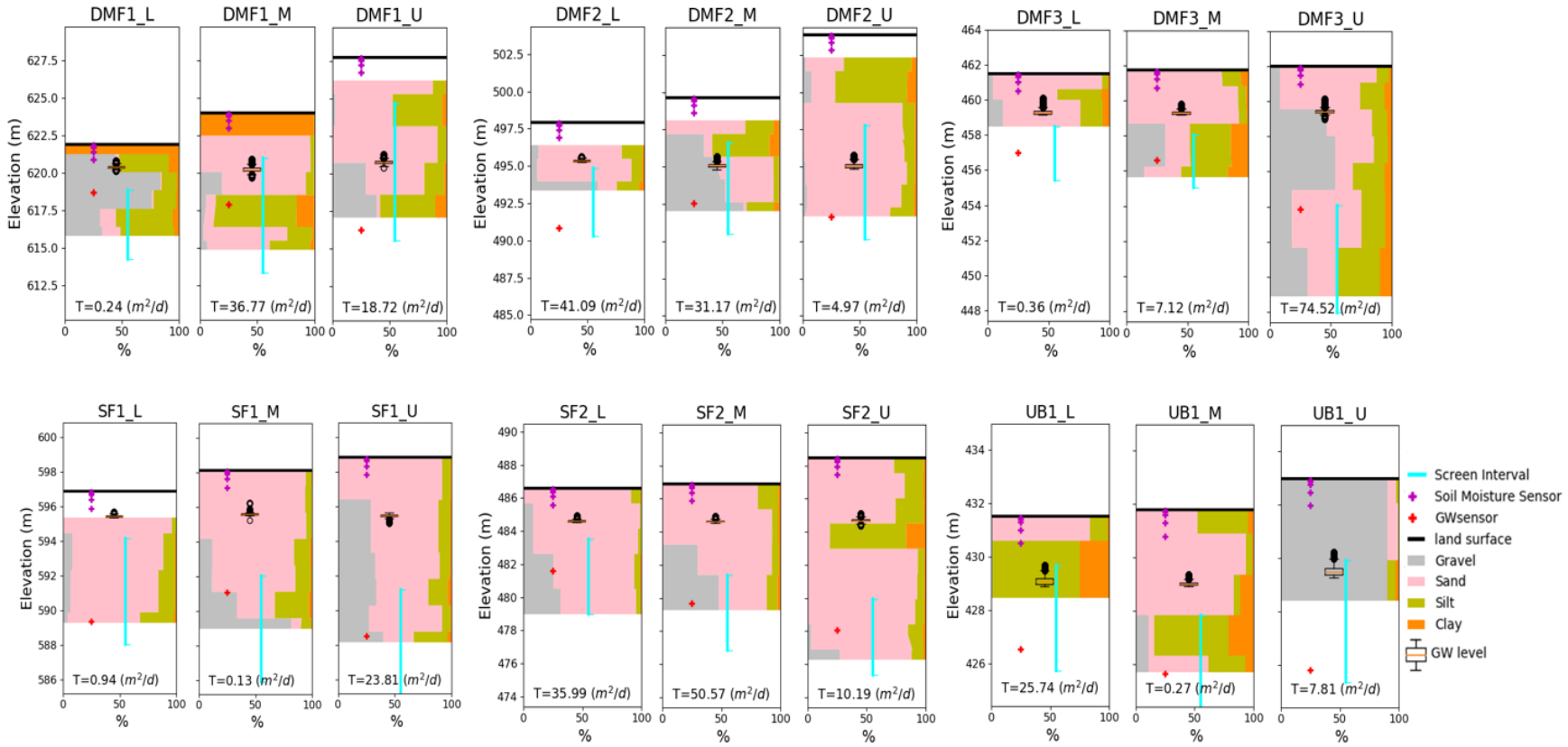

Figure 6. Experimental layout with monitoring wells, soil and groundwater sensors, and generalized soil type.

Soil-particle size distribution, aquifer transmissivity, screen interval, depths of soil and groundwater sensors, and groundwater elevation are also shown. DMF: Double Mountain Fork, SF: Salt Fork, UB: Upper Brazos. U: upper terrace well, M: middle terrace well, L: lower terrace well. GW: groundwater, T: transmissivity.

our study period was from November 2017 to September 2018, when precipitation was lower and summer 2018 when evaporation was elevated. After September 2018, the amount of soil-water storage increased at all locations from early fall rain showers and lower evaporation and plant water consumption through the winter months.

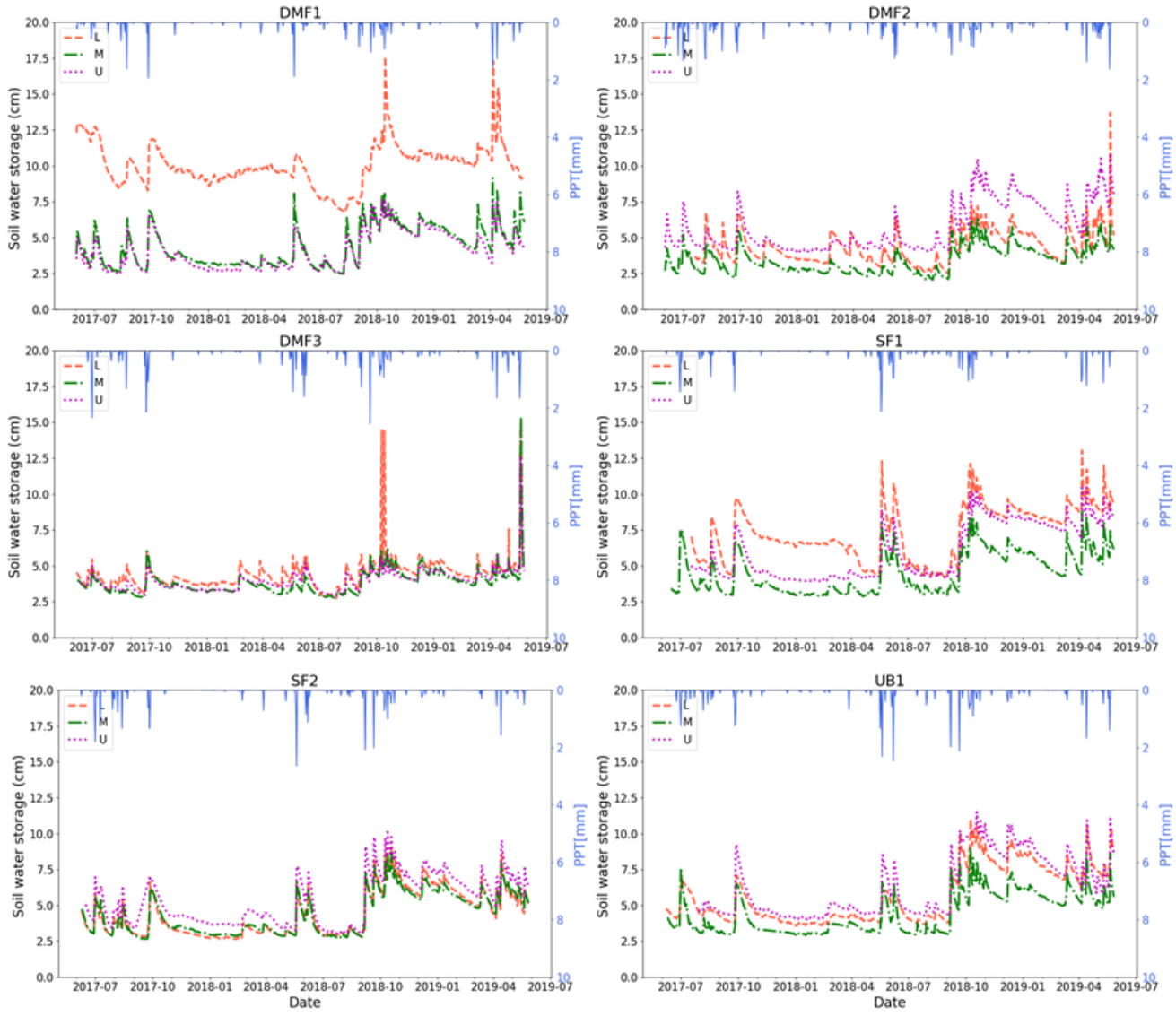

Figure 7. Soil-water storage.

Precipitation at each location shown at top of each figure. Red: Lower well, Green: Middle well, Purple: Upper well. DMF: Double Mountain Fork, SF: Salt Fork, UB: Upper Brazos. U: upper terrace well, M: middle terrace well, L: lower terrace well.

4.4 Soil evapotranspiration and root water uptake

To evaluate the potential effects of saltcedar control activities on soil and alluvial water storage, we assessed diurnal fluctuations of soil moisture to estimate soil ET. We found that plant transpiration fluctuations in total soil moisture at 50-cm depth is only detectable at the UB1 upper-well location (Figure 8), where there was not aerial applications of saltcedar treatment directly on the site, in addition to the SF2 and UB1 middle wells. Diurnal fluctuations in volumetric soil-water content of these sites showed water extraction during dry weather conditions (i.e., when soil moisture from rainfall was not available), which could be attributable to ET from saltcedar or other riparian vegetation. Figure 9 shows daily actual ET changes during dry periods (i.e., time periods with precipitation were omitted) at three sites where effects of ET on diurnal soil-water changes were observed. Actual ET amounts were less than 1 cm/day during the study period. Maximum values of ET were observed between June and July.

4.5 Groundwater evapotranspiration

At our sites, groundwater is found at depths less than 3 m (box plots in Figure 6). Results of groundwater ET estimation using the White (1932) method are presented on Figure 10. The vertical line in some figures represents the middle of the saltcedar treatment period where treatment occurred.

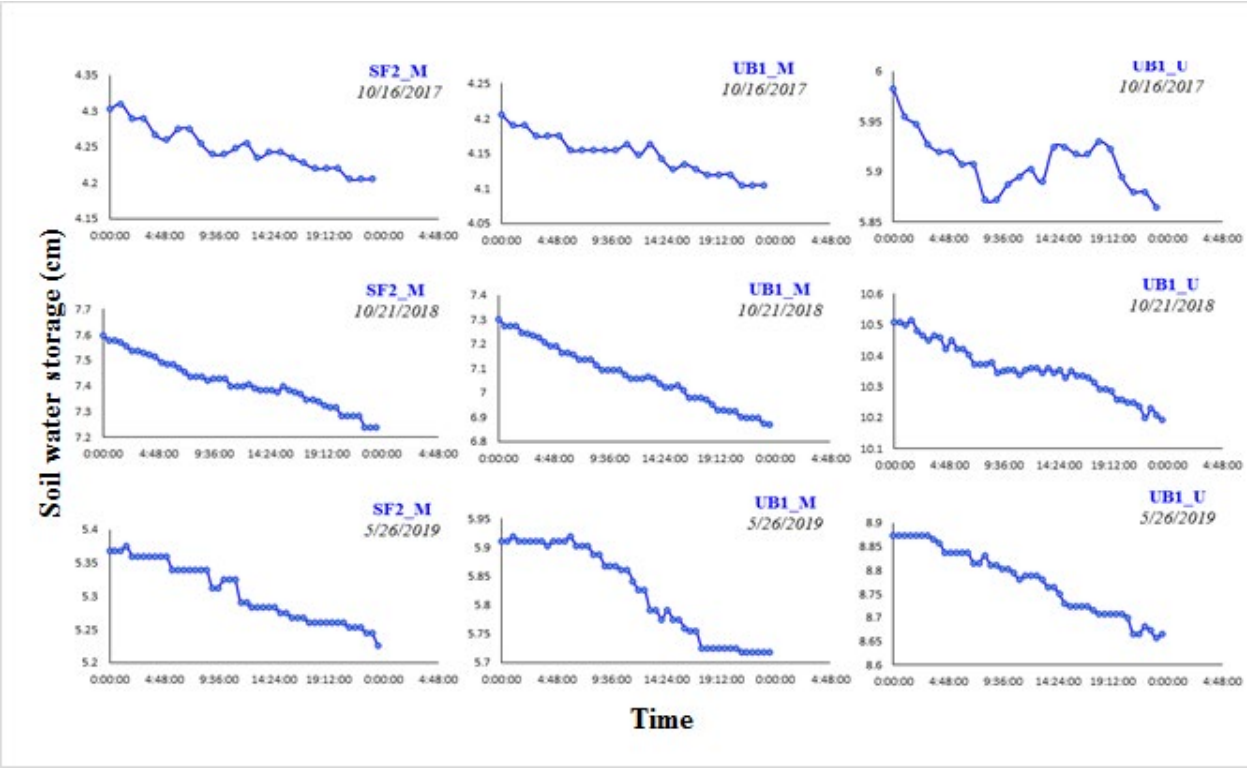

Figure 8. Daily total soil moisture fluctuations at SF2_M, UB1_M, and UB1_U (Oct. 2017, Oct. 2018, and May 2019).

Soil water storage shown is measured through 50 cm depth.

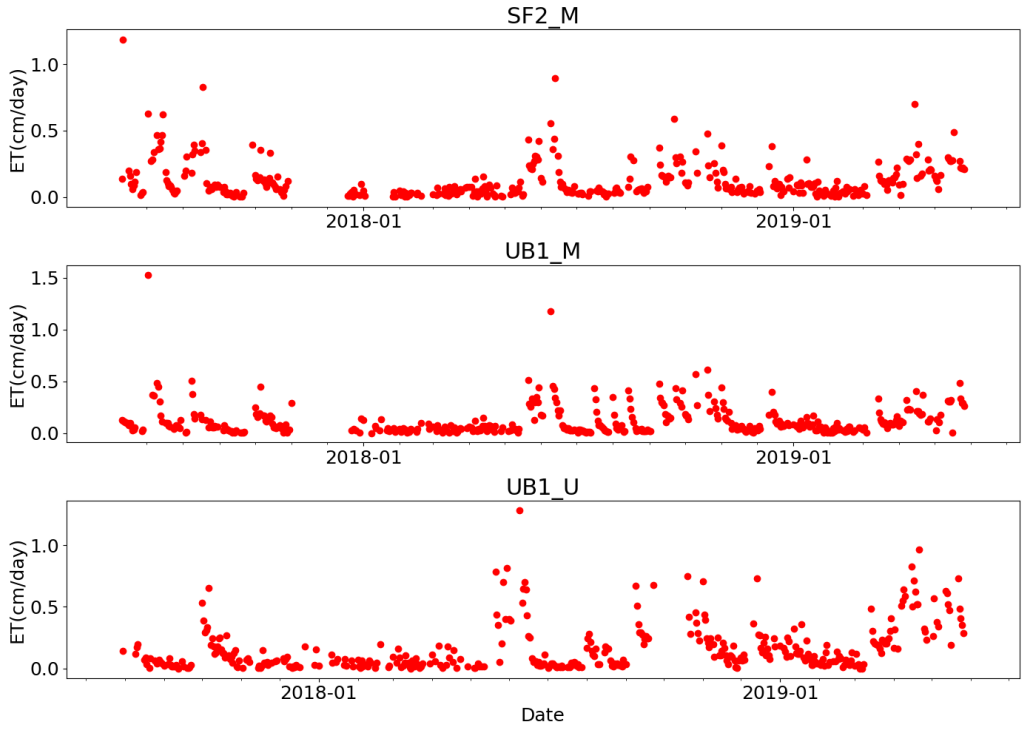

Figure 9. Soil ET variations at locations where diurnal transpiration was observed.

SF: Salt Fork, UB: Upper Brazos.

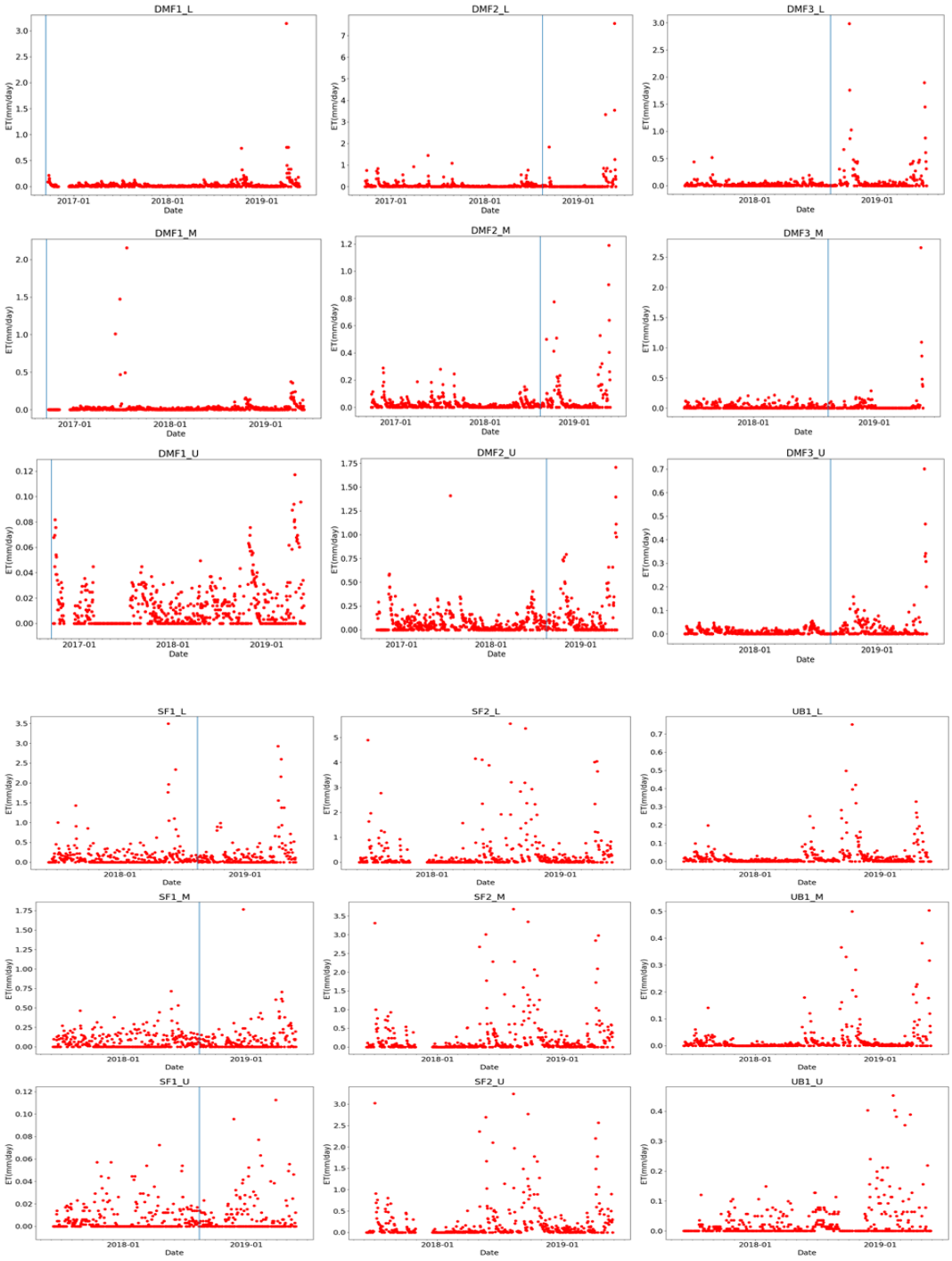

Figure 10. ET_g changes using modified White (1932) method.

Vertical blue lines show middle of saltcedar aerial treatment time (June–Sept., 2018) at each location. DMF: Double Mountain Fork, SF: Salt Fork, UB: Upper Brazos.

At DMF1, ET_g was close to zero at all three monitoring wells at this site. ET_g at DMF1_U was always less than 0.12 mm/day. At the DMF2 and DMF3 sites, the lower and nearest monitoring wells to the river (DMF2_L and DMF3_L) had more ET_g (from 0 to 7 mm/day and from 0 to 3 mm/day, respectively) than the other two wells at each of these sites. Importantly from a standpoint of assessing efficacy of herbicide treatment on saltcedar water use, one year after saltcedar treatment, the amount of ET_g had not decreased.

At the SF1 site, values of ET_g also did not change after the 2018 treatment. The range of ET_g values was greater at SF1_L, ranging from 0 to 3.5 mm/day. With increased distance from the river, at SF1_M and SF1_U, the amount of ET_g decreased, likely due to the difficulty of roots accessing the deeper groundwater at the higher wells. The lowest amount of ET_g at this location was at the SF1 upper well, with less than 0.12 mm/day.

The SF2 site upstream did not have saltcedar treatment during our study period. The range of ET_g changes was greater at the lower well than at the two other middle- and upper-terrace wells. The value of ET_g was between 0 to 5 mm/day at SF2_L and less than 3.5 mm/day for SF2_M and SF2_U wells. The values of ET_g was greater during spring and summer.

The value of ET_g at the UB1 site was lowest, less than 0.7 mm/day at UB1_L. ET_g decreased with increasing distance from the river at the UB1_M and UB1_U wells, which were less than 0.5 mm/day and 0.4 mm/day, respectively. The highest amounts of ET_g were observed during spring and summer.

ET_g estimation results from our study sites showed that at the DMF1 site, the ET_g was low; but because the monitoring started after the first treatment, we cannot compare the effect of saltcedar treatment at this site. For the other three sites treated during 2018, we have results of

71 estimated ET_g from before and after treatment; however, we could not detect any ET_g trend
72 changes after only one year because saltcedar is a perennial plant with deep roots, and the effects
73 of treatment may need more time to be appear. For the two sites without treatment (SF2 and UB1)
74 the value of ET_g was highest during spring and summer of 2018 and 2019. Our results suggest that
75 ET_g is already quite low, and we may not expect substantial water salvage to support instream
76 flows following additional herbicide application under the current saltcedar plant density
77 monitored at our study sites.

78 **4.6 Alluvial water storage**

79 Alluvial aquifer water storage in our study area varies from 0 to 0.8 m of groundwater equivalent
80 depth water depth (i.e., depth of column of water at a particular well accounting for porosity).
81 Alluvial recharge occurred during precipitation and elevated streamflow during floods; the greatest
82 available storage was during June 2019, as well as during November and December 2019 (Figure
83 11). Figure 11 shows that the highest streamflow events result in much more alluvial recharge and
84 a longer persistence of floodwater in the subsurface than what occurred after smaller flows
85 following lighter precipitation. For example, at DMF3, rain in the fall of 2018 increased
86 groundwater storage for at least 6 months until the next round of heavy precipitation began in
87 spring 2019. However, during the same time period, DMF1 and DMF2 located further upstream
88 did not have as much of an increase in groundwater storage, suggesting that higher flows that may
89 occur more often at downstream basin locations may be more important for alluvial aquifer
90 recharge. Also, streamflows on SF do not appear to be high enough to result in appreciable
91 near-stream groundwater recharge during floods we monitored. Simpson et al. (2011) reported
92 that only the largest and longest precipitation events caused observable changes in both baseflow

volume and the composition of baseflow and riparian groundwater, which is consistent with our findings.

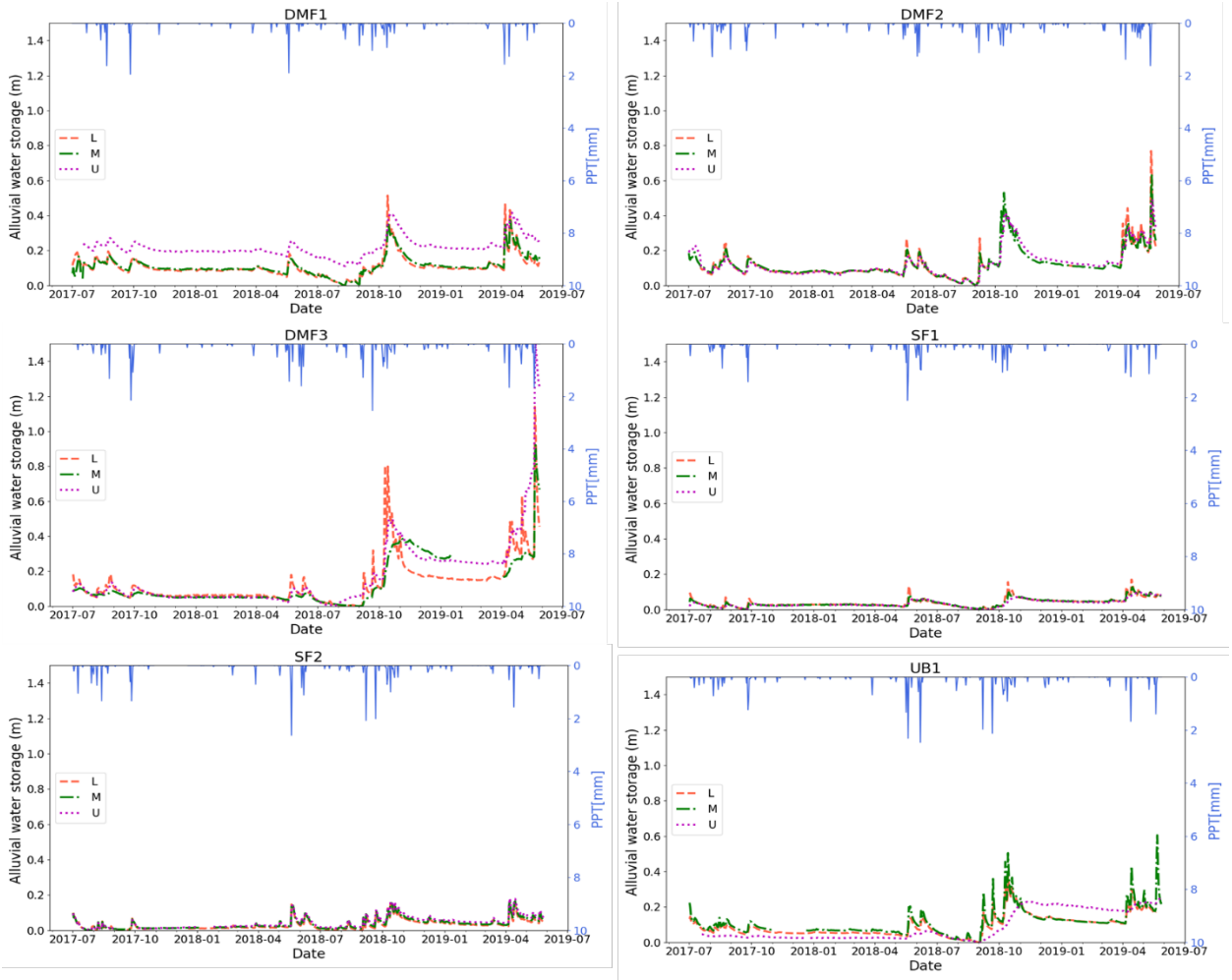

Figure 11. Alluvial aquifer groundwater storage time series.

Red: Lower well, Green: Middle well, Purple: Upper well. DMF: Double Mountain Fork, SF: Salt Fork, UB: Upper Brazos. U: upper terrace well, M: middle terrace well, L: lower terrace well.

The number of increases in alluvial aquifer groundwater levels for lower, middle, and upper wells at locations DMF2, SF1, and SF2 were similar. Alluvial water-storage minimum and maximum values had trends similar to soil- water storage and dry periods of November 2017 to September 2018—the minimum values of alluvial storage. The amount of alluvial water storage increased after precipitation events from mid-September to November 2018 at all sites, then decreased during dry periods until April 2019. However, the amount of alluvial storage during these dry periods was more than the amounts of alluvial water storage during previous dry periods, suggesting that antecedent alluvial aquifer storage conditions are important to recharge processes (Figure 11). Thus, following prolonged drought, it would be expected that renewed streamflows may be lost to replenish a relatively dry alluvial aquifer. Also, alluvial groundwater storage at the DMF3 lower well increased more than at middle and upper wells after each precipitation event, reflecting the lower well's closer position to the stream. However, during dry periods, water storage decreases more at this location because of the effects of soil ET on shallow groundwater there.

4.7 Groundwater hydraulic gradients and flux

Our evaluation of alluvial aquifer groundwater hydraulic gradient and flux reveals that flow-direction and flux magnitude changes over time with different types and duration of precipitation events and subsequent increases in streamflow (Figure 12). We characterized how different levels of streamflow ("low", "medium", and "high" flows) affect alluvial aquifer groundwater flow direction and flux using cumulative distribution functions (CDF) of discharge data of the closest USGS gage to a particular site (1940–2019 stream discharge). We used USGS Seymour gage discharge data for the UB1 site and DMF Aspermont and SF Aspermont gages for DMF (DMF1,

DMF2, DMF3) and SF (SF1 and SF2) sites. We categorized the resulting CDFs into three groups: low flow (which occurred less than 25 percent of the time), median flow (0.25—0.75 CDF), and high flow (>0.75 CDF). Our analysis revealed that for the sites we monitored, groundwater flow direction and flux are remarkably consistent, only changing during the highest flows following heavier precipitation. Changes in gradient and flux also become more pronounced the further downstream in DMF and are almost absent in SF during the study period.

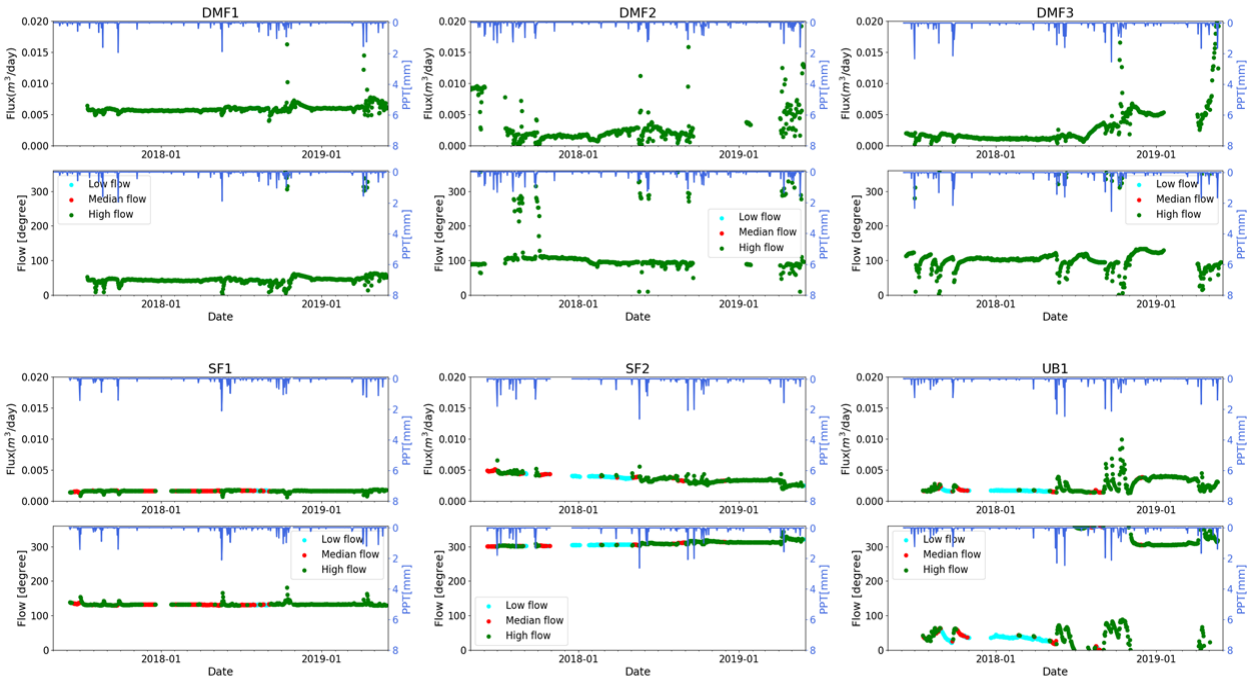

Figure 12. Groundwater hydraulic gradient during low, median, and high upstream flows. Blue: Low streamflow, Red: Median streamflow, Green: High streamflow. Streamflow classification based on cumulative distribution functions (CDF) of historic (1940–2019) USGS gauge data with CDFs divided into three groups: low flow (which occurred less than 25 percent of the time), median flow (0.25–0.75 CDF), and high flow (>0.75 CDF). DMF: Double Mountain Fork, SF: Salt Fork, UB: Upper Brazos. U: upper terrace well, M: middle terrace well, L: lower terrace well.

Figure 13 shows groundwater hydraulic gradient magnitude and direction at each location during the study period, using a rose diagram. Various colors indicate the magnitude of groundwater hydraulic gradient (mm/m) and its direction. Numbers of each circle inside the rose diagram indicate the time frequency of each direction (i.e., from 0 to 100 percent of the time).

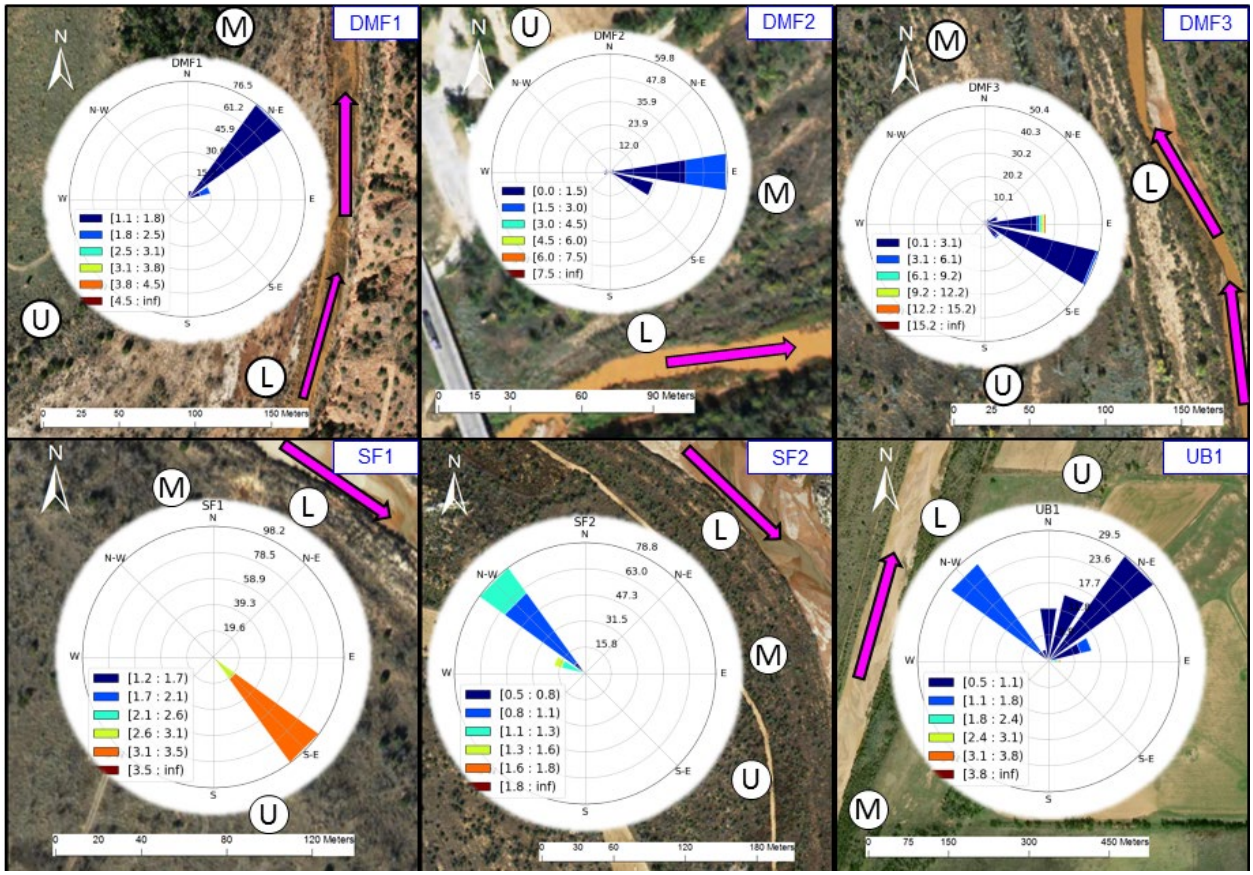

Figure 13. Groundwater hydraulic magnitude and flow direction.

Colors and legend show hydraulic magnitude in mm/m. Numbers inside circles show the frequency that each gradient magnitude and direction occurs. Pink arrows show streamflow direction. L, M, and U represent lower, middle, and upper terrace monitoring wells, respectively. DMF: Double Mountain Fork, SF: Salt Fork, UB: Upper Brazos.

At DMF1, flux changes were minor (~0.005 m^3/day; Figure 12). Hydraulic gradient magnitude was between 1.1 and 2.5 mm/m (Figure 13). During 100 percent of our study period, flow direction was essentially parallel and the river alluvium conveyed groundwater through the point bar. Net flows to the river from the alluvium ~92 percent of the time could be attributed to flows through sands and gravels of the relatively long point bar (~1.4 km) from upstream to downstream locations and not necessarily actual groundwater inflows from surrounding aquifers (Figure 13). Additional monitoring well date farther from the stream would be needed to better characterize non-alluvial aquifer groundwater inflows to the stream.

At DMF2, flux and hydraulic gradient variation were greater (between 0 to 0.015 m^3/day and 0 to 3 mm/m, respectively). Flow direction was parallel to the river about 77 percent of the time and toward the river 23 percent of the time. About 7 percent of the time, a reversal of flow direction was observed at this location during higher-flow events (Figure 13).

Among study sites, DMF3 had the maximum changes in flux (0–0.02 m^3/day) and hydraulic gradient magnitude (0–12.2 mm/m) (Figure 12). In all of our study periods, the flow direction of DMF3 changed, but the groundwater gradient was toward the river (Figure 13).

At SF1, hydraulic gradient magnitude and flow direction did not change appreciably; the magnitude was between 2.6 and 3.5 mm/m, and the direction was always parallel to the river (Figure 13). SF1 hydraulic gradient in 95 percent of the study period was between 0.8 and 1.3 mm/m. Oddly, at SF2, groundwater flow direction is opposite the flow direction of the river, which might be explained by the nearly linear monitoring well configuration (instead of the idea triangular configuration) not accurately characterizing local groundwater conditions (Figure 13).

172 At the UB1 site, the change of the flow direction was greater than at other sites. Water
173 sloped toward the river 25 percent of the time with a hydraulic gradient magnitude between 1.1
174 and 1.8 mm/m. Most of the time, however, the hydraulic magnitude was between 0.5 and
175 1.1 mm/m, and the flow direction was parallel to the river. The groundwater hydraulic gradient
176 was greater during high streamflow and precipitation events, and flow direction was from river to
177 aquifer at this downstream site. During median and low streamflow, the hydraulic gradient was
178 relatively stable. The majority of the time, flow direction during low flow was from the alluvial
179 aquifer to river. As with SF2, the relatively linear monitoring well configuration at UB1 (due to
180 site constraints) may add uncertainty to interpretation of localized groundwater flux.
181 The flow direction at our UB study sites indicates that the alluvial storage is somewhat
182 important following elevated streamflows; however, alluvial aquifer groundwater levels during the
183 study period receded to pre-flood conditions within a few weeks or months. Most of the time,
184 groundwater in the alluvial aquifers is moving roughly parallel to the river. Recharge to the aquifer
185 also occurs from downward percolation of rainfall to the saturated zone and more importantly
186 when streamflow is elevated. In alluvial aquifers with high hydraulic conductivity the
187 groundwater gradients between the stream and alluvium usually are not large; however, the amount
188 of surface water-groundwater exchange can be considerable. Conversely, when hydraulic
189 conductivity is low, the gradients between the stream and the groundwater system generally are
190 large, but the amount of water exchanged between the two water compartments regularly is small
191 (Winter et al., 1998). In our study area, our monitoring results suggest the former, with the alluvial
192 aquifer closely connected to its stream.

193 Reversed hydraulic gradients observed a small percentage of the time at UB1 and DMF2
194 (Figure 13) can induce flow from the stream channel into the riparian zone. These reversed
195 hydraulic gradients may exert a strong influence on riparian zone vegetation dynamics and
196 subsurface biogeochemistry (Duval and Hill, 2006). Previous studies have measured the timing
197 and driving forces of volumetric fluxes of subsurface water to rivers and differences in hydraulic
198 gradient between aquifer and river. Results of these studies showed that most discharge from the
199 alluvial aquifer to the stream occur immediately following storm events (Unland et al., 2013; Yu
200 et al., 2013). Our monitoring data suggest that the alluvial aquifers in the study area are recharged
201 rapidly during elevated streamflow and subsequently release water relatively rapidly to contribute
202 to streamflow for weeks or months, instead of the multi-year groundwater outflows observed by
203 Simpson et al. (2013) from alluvial aquifers following floods in the Bill Williams River in Arizona.
204 Figure 14 shows correlations of high, median, and low streamflow with the average alluvial
205 aquifer storage of the three wells at each location. Low streamflow is highly correlated with
206 average aquifer alluvial storage at most locations, suggesting that the alluvial aquifer is well
207 connected to the river. This assertion is supported by elevated hydraulic conductivity values
208 measured during monitoring well slug tests indicative of highly-transmissive sand and gravel
209 (Figure 6). Flow direction through the riparian zone was parallel to the stream at most study
210 locations during low stream stages and the groundwater table (Figure 12, Figure 13). At the UB1
211 site, the river gaining/losing water from/to the aquifer varies depending on season and stream
212 stage. The high correlation ($R^2 = 0.91$) between alluvial storage and low streamflow that occurs
213 during dry periods shows that the stream stage and alluvial storage are low. During high

streamflow with precipitation events, a lower correlation ($R^2 = 0.47$) between alluvial storage and streamflow exists (Figure 14).

Figure 15 presents an evaluation of baseflow, storm flow, and total streamflow at the USGS Seymour gage compared to the sum of streamflow at upstream DMF and SF Aspermont gages. This analysis of long-term streamflow (January 2017–May 2019) can be used to infer groundwater inflows (in addition to surface water inflows from smaller, ungauged catchments) between the Aspermont gauges and Seymour. Baseflow for USGS upstream gauges were always less than 2.5 m^3/s from 2017 (after 1 year of saltcedar treatment) to 2019.

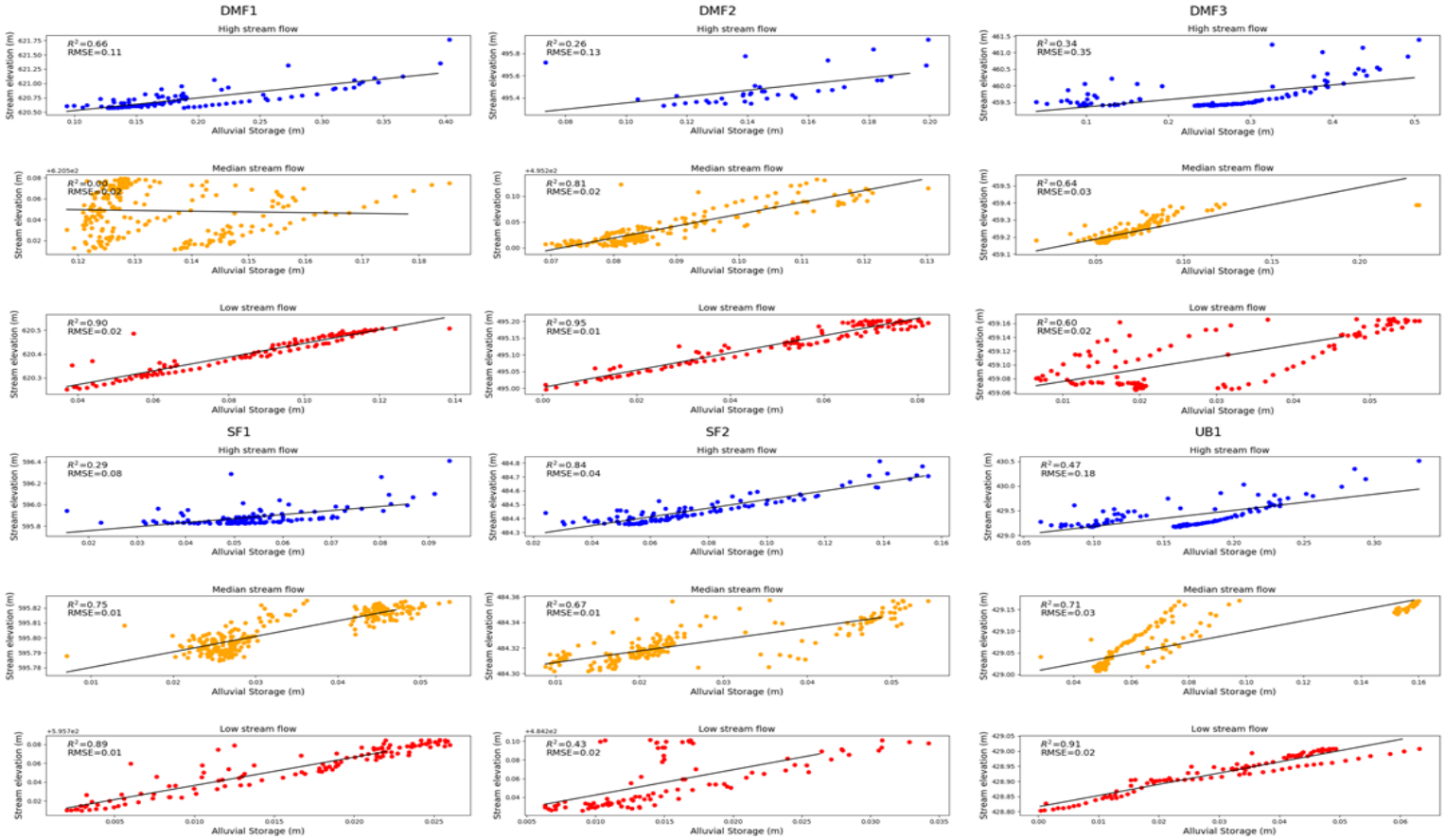

Figure 14. Correlation between stream stage and alluvial storage.

Red: Low streamflow, Yellow: Median streamflow, Blue: High streamflow. DMF: Double Mountain Fork, SF: Salt Fork, UB: Upper Brazos.

Of interest, the baseflow, storm flow, and total streamflow analysis reveals that the stream was losing water to the alluvial aquifer (or evaporation) from summer to fall 2017 when streamflow pulses were lower magnitude and shorter duration compared to higher streamflow from mid-2018 to mid-2019 (Figure 15). Also of interest is that during this period, precipitation was not sufficiently intense to generate streamflow (Figure 8); however, our evaluation of soil ET shows that the precipitation was heavy enough to provide shallow, root-accessible moisture for riparian vegetation (Figure 9), but ET_g was minimal (Figure 9), suggesting groundwater was too deep for vegetation to easily access. After September 2018, baseflow, storm flow, and total flow increased. During this same time period, we also observed an increase in soil and alluvial water storage. As with Simpson et al. (2013), our study suggests that floods need to be of a sufficient magnitude (perhaps, per Figure 14, at least 25–50 m^3/sec [880–1760 ft^3/sec]) and duration to overcome antecedent moisture deficits and results in sustained streamflow, alluvial aquifer recharge, and subsequent baseflow contributions to streams. Additional research is needed to refine antecedent conditions, as well as flood magnitude and duration, which cause loss of streamflow to alluvial aquifers. To this end, it would be good to compare flood peak and climatic conditions during our study period to the historical record to understand if higher floods under pre-development natural flow regime may have resulted in additional alluvial aquifer storage and subsequent flows to the stream during dryer conditions (i.e., summer and drought). Our study results indicate that groundwater flows to UB streams from alluvial aquifers under the streamflow regime observed during our study period lasted much shorter (weeks to months) than the multi-year, post-flood groundwater flows in a Western United States stream that Simpson et al. (2013) observed.

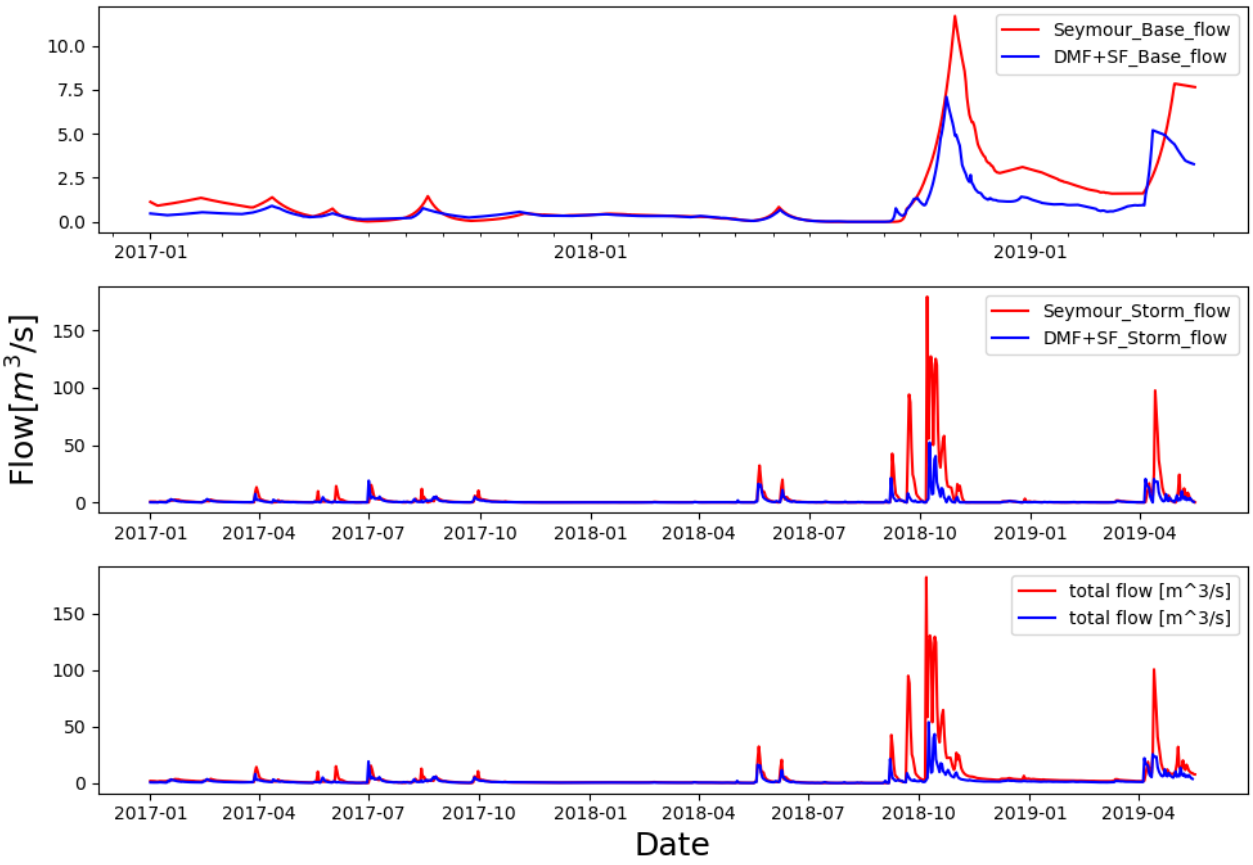

Figure 15. Baseflow, storm flow, and total streamflow (2017–2019).

Data shown are flows at Seymour USGS gauge minus the sum of flows at the USGS DMF and SF Aspermont gauges. For the top figure, when red line is above the blue line, the stream is gaining flows from the Seymour Aquifer and ungauged smaller catchments. When the red line is below the blue line, the stream is losing water to alluvial aquifer storage, evapotranspiration, and other losses between the two headwater gauges and Seymour.

4.8 Assumptions and limitations of this approach

We assume that all measured data are accurate (i.e., soil moisture, groundwater, streamflow) and that our integration of soil moisture in the near surface provides an accurate estimate of total soil moisture water storage. We are limited by the number of groundwater monitoring wells at each

location; thus, we assume our evaluation of groundwater ET use, hydraulic gradient, and groundwater flux accurately represent local groundwater conditions. This study is also limited by the data prior to and post salt cedar treatment and the fact that saltcedar is a perennial plant. An additional limitation includes sparse monitoring locations which we assume accurately represent basin-scale hydrologic processes in the stream and associated alluvial aquifer.

4.9 Previously reported hydrologic modeling

We also previously reported the results of a hydrologic model of the DMF that we implemented using the Coupled Routing and Excess STorage (CREST) model in the Draft Final Report submitted October 6, 2017. The objective of the model was to simulate potential increases in baseflow following cedar abatement. The model was first calibrated to USGS discharge data at Aspermont and Justiceburg. Abatement was simulated using a reduction in leaf-area indices along the riparian corridor of the DMF at 10, 20, 50 and 75%. This corresponds to a treatment area of 97,000 acres upstream of Aspermont and 24,000 acres above Justiceburg. The average modeled annual increase in water yield was 602 and 1,157 gal/acres for the Aspermont and the Justiceburg watershed, respectively, with a 10% reduction in leaf-area. Water yields increased to 18,705 and 36,758 gal/acre with a 75% leaf-area reduction. The model captured monthly and annual cycles well, but peak flows—which this study finds are important for basin-scale hydrologic processes—were poor. Two potential limitations of the previous model are that large cell size (1 km^2) to accurately represent smaller-scale stream-groundwater interactions and that the CREST model itself does not evaluate groundwater flows with much finesse.

4.10 Future work

We recommend that ongoing hydrologic monitoring be continued and include time for equipment maintenance and data analysis. While the results to date suggest that effects of herbicide application to saltcedar stands has not yet resulted in appreciable reduction of ET in the soil moisture or groundwater, this analysis has some caveats, which include that (1) some monitoring sites were not directly treated with herbicide, (2) treatment varied spatially and temporally during each of the three years of treatment occurred, and (3) the study presents a relatively short monitoring period prior to and following treatment with most sites treated in 2018 and data used in this study was until May 28, 2019 before peak ET usually occurs.

Future work when comparing ET should not focus on times when saltcedar would be dormant through the winter months. However, groundwater and surface water development will continue in the UB and it is important to understand how it may affect basin hydrology into the future. In addition, one important application of saltcedar abatement efforts in the UB is the potential to restore stream geomorphology to more natural conditions. To this end, research on the Rio Puerco of New Mexico found that following herbicide application, a subsequent intense flood was able to scour dead saltcedar and reconfigure stream geomorphology an >80% wider mean channel width in sprayed reaches (Perignon et al., 2013; Vincent et al., 2009). If ongoing saltcedar abatement efforts and hydrologic monitoring are continued and such a flood were to occur in the UB, we would then have the hydrologic data needed to assess how pre- and post-flood new stream geomorphology may affect surface water-groundwater interactions. An additional possibility for future work is refinement of the current hydrologic model or development of a new hydrologic model that is able to more effectively represent reach-scale stream-groundwater interactions. A

refined model thus could potential be able to understand flooding, bank storage, and alluvial aquifer drainage process we identified in this study more effectively—under the current flow regime and possible future stream geomorphology following floods such as that on the Rio Puerco of New Mexico.

5 Conclusions

We developed an extensive hydrologic monitoring network at six locations in the UB basin for three years, during which herbicide was applied to control treatment invasive saltcedar. The primary results of the study are:

- Alluvial aquifers are comprised of highly transmissive sands and gravels, permitting relatively rapid stream-groundwater exchanges, generally flat water table conditions, and groundwater flow parallel to stream during most flow conditions. Groundwater gradients changed during flows that occur only ~25 percent of the time (based on period of record of 1940 to 2019).
- Our estimates of ET of riparian vegetation calculated using diurnal fluctuations soil moisture and groundwater found that ET is less and 1 cm/day and we could not discern changes in ET before or after herbicide application to saltcedar stands. However, most sites were treated in 2018 and data used in this study was until May 28, 2019 before peak ET usually occurs. Thus—consistent with recent research (Wilcox et al., 2006)—any continued saltcedar control efforts are unlikely to salvage appreciable water.
- From summer to fall 2017, streamflow pulses were low-magnitude and did not recharge the alluvial aquifer. During this time, our soil moisture ET analysis suggested riparian vegetation were able to access soil moisture following rains that were insufficiently heavy to result in

much streamflow, but ET from groundwater was minimal because groundwater was too deep for most vegetation to easily access.

- Monitoring at locations more upstream (i.e., DMF1 and DMF2) had less variability in alluvial aquifer storage, suggesting that higher flows which occur more often at downstream basin locations be may needed for alluvial aquifer recharge. Our analysis of USGS stream gauges suggest that floods of at least 25–50 m^3/sec [880–1760 ft^3/sec] may be needed to overcome any antecedent moisture deficits in the alluvial aquifer and streambed and result in recharge of alluvial aquifers.
- Similarly, our analysis of baseflow found that streams lost water in 2017, a period of relatively low flood pulses (i.e., <25 m^3/sec, or 880 ft^3/sec), which suggests that following a particularly dry summer or prolonged drought, initial renewed streamflows may be lost to replenish dry alluvial aquifers and stream beds.
- Conversely to Simpson et al. (2013), who found that floods on a similar aridland stream system result in sufficient alluvial aquifer recharge to provide baseflows that maintain streamflows for years, floods we observed during the study period appear to only provide drainage to the stream for weeks to months. Furthermore, as upstream reservoirs impound most streamflow, floods from the farthest upstream portions of the UB basin only progress downstream once upstream reservoirs are full. Also, consistent with other studies, most discharge from the alluvial aquifer to the stream occurs soon after storm events when groundwater gradients between the alluvial aquifer and stream are greatest (Unland et al., 2013; Yu et al., 2013). The objective of separate, concurrent, TPWD-funded study in the UB basin is to evaluate how groundwater development,

dam construction, and climatic variability has affected the flow regime (e.g., floods, baseflow, etc.) needed for aquatic ecosystem health.

- Our evaluation of soil ET shows that the precipitation was sufficient to provide shallow, root-accessible moisture for riparian vegetation, but ET_g was minimal (Figure 9), suggesting groundwater was too deep for vegetation to easily access during most of the study period.

Continued hydrologic monitoring in the basin would provide the data needed to further understand the role of groundwater-surface water interactions in supporting riparian vegetation ET and stream baseflows. In addition, updated hydrologic modeling could be done to understand stream-groundwater interactions under the current and potential future flow regimes and geomorphology.

6 Acknowledgements

Thanks to Monica McGarrity (TPWD), Kevin Mayes (TPWD), and Omar Bocanegra (USFWS) for helpful discussions and technical support; Karim Aziz (TPWD) for surveying well elevations; Duane Lucia (USFWS) for landowner outreach and numerous private landowners who graciously made this study possible; and C. Breton (UT-BEG) for help with data collection, processing, and mapping; Ali Forghani (Intera Inc.) for technical support on Python scripting.

7 Funding information

Support for this study to UT-BEG was provided in part by TPWD (TPWD Contract No. 505176, “Monitoring of Hydrologic Effects of Salt Cedar Control in the Upper Brazos River Basin, Texas”) and The University of Texas at Austin Jackson School of Geosciences.

8 References

Baker, R., Hughes, L. S., and Yost, I., 1964, Natural Sources of Salinity in the Brazos River, Texas, with particular referece to the Croton and Salt Croton Creek Basins. U. S. Geological Survey Water-Supply Paper 1669-CC. Prepared in cooperation with the Brazos River Authority.

Baldys, S., III, and Schalla, F. E., 2011, Baseflow (1966–2009) and Streamflow Gain and Loss (2010) of the Brazos River from the New Mexico–Texas State Line to Waco, Texas. Prepared in cooperation with the Texas Water Development Board. U.S. Geological Survey Scientific Investigations Report 2011–5224.

Blackburn, W., Knight, R., and Schuster, J., 1982, Saltcedar influence on sedimentation in the Brazos River: Journal of Soil and Water Conservation, v. 37, no. 5, p. 298-301.

Bouwer, H., and Rice, R., 1976, A slug test for determining hydraulic conductivity of unconfined aquifers with completely or partially penetrating wells: Water resources research, v. 12, no. 3, p. 423-428.

Brune, G. M., 2002, Springs of Texas, Texas A&M University Press.

Busby, F. E., and Schuster, J. L., 1973, Woody phreatophytes along the Brazos River and selected tributaries above Possum Kingdom Lake. Texas Water Development Board Report 168, p. 50.

Clothier, B. E., and Green, S. R., 1994, Rootzone processes and the efficient use of irrigation water: Agricultural Water Management, v. 25, no. 1, p. 1-12.

Dean, D., Scott, M., Shafroth, P., and Schmidt, J., 2011, Stratigraphic, sedimentologic, and dendrogeomorphic analyses of rapid floodplain formation along the Rio Grande in Big Bend National Park, Texas: Geological Society of America Bulletin, v. 123, no. 9-10, p. 1908-1925.

Doble, R., Brunner, P., McCallum, J., and Cook, P. G., 2012, An analysis of river bank slope and unsaturated flow effects on bank storage: Groundwater, v. 50, no. 1, p. 77-86.

Doody, T. M., Nagler, P. L., Glenn, E. P., Moore, G. W., Morino, K., Hultine, K. R., and Benyon, R. G., 2011, Potential for water salvage by removal of non-native woody vegetation from dryland river systems: Hydrological Processes, v. 25, no. 26, p. 4117-4131.

Duval, T., and Hill, A., 2006, Influence of stream bank seepage during low-flow conditions on riparian zone hydrology: Water Resources Research, v. 42, no. 10.

Evermann, B. W., and Kendall, W. C., 1894, The fishes of Texas and the Rio Grande basin, considered chiefly with reference to their geographic distribution, US Government Printing Office.

Fahle, M., and Dietrich, O., 2014, Estimation of evapotranspiration using diurnal groundwater level fluctuations: Comparison of different approaches with groundwater lysimeter data: Water Resources Research, v. 50, no. 1, p. 273-286.

Freeze, R. A., and Cherry, J. A., 1979, Groundwater: Englewood Cliffs: New Jersey.

Gribovszki, Z., Szilágyi, J., and Kalicz, P., 2010, Diurnal fluctuations in shallow groundwater levels and streamflow rates and their interpretation–A review: Journal of Hydrology, v. 385, no. 1-4, p. 371-383.

Guderle, M., and Hildebrandt, A., 2015, Using measured soil water contents to estimate evapotranspiration and root water uptake profiles–a comparative study: Hydrology and Earth System Sciences, v. 19, no. 1, p. 409-425.

Heath, R. C., 1998, Basic ground-water hydrology. U.S. Geological Survey Water-Supply Paper 2220.

Hupet, F., Lambot, S., Javaux, M., and Vanclooster, M., 2002, On the identification of macroscopic root water uptake parameters from soil water content observations: Water Resources Research, v. 38, no. 12, p. 36-31-36-14.

Loheide, S. P., Butler Jr, J. J., and Gorelick, S. M., 2005, Estimation of groundwater consumption by phreatophytes using diurnal water table fluctuations: A saturated-unsaturated flow assessment: Water resources research, v. 41, no. 7.

Loheide, S. P., II, 2008, A method for estimating subdaily evapotranspiration of shallow groundwater using diurnal water table fluctuations: Ecohydrology: Ecosystems, Land and Water Process Interactions, Ecohydrogeomorphology, v. 1, no. 1, p. 59-66.

Malvern, 2013, Mastersize 3000 User Manual.

Mazor, E., and Nativ, R., 1992, Hydraulic calculation of groundwater flow velocity and age: examination of the basic premises: Journal of Hydrology, v. 138, no. 1, p. 211-222.

McDonald, A. K., Sheng, Z., Hart, C. R., and Wilcox, B. P., 2013, Studies of a regulated dryland river: surface–groundwater interactions: Hydrological Processes, v. 27, no. 12, p. 1819-1828.

McDonald, A. K., Wilcox, B. P., Moore, G. W., Hart, C. R., Sheng, Z., and Owens, M. K., 2015, Tamarix transpiration along a semiarid river has negligible impact on water resources: Water Resources Research, v. 51, no. 7, p. 5117-5127.

McGarrity, M. E., 2017, Aerial helicopter surveys of saltcedar density.

-, 2019, Saltcedar imazapyr treatment dates and locations.

Meyboom, P., 1967, Ground Water Studies in the Assiniboine River Drainage Basin: Hydrologic Characteristics of Phreatophytic Vegetation in South-Central Saskatchewan, Department of energy, mines and resources.

Nachabe, M. H., 2002, Analytical expressions for transient specific yield and shallow water table drainage: Water resources research, v. 38, no. 10, p. 11-11-11-17.

Nagler, P. L., Shafroth, P. B., LaBaugh, J. W., Snyder, K. A., Scott, R. L., Merritt, D. M., and Osterberg, J., 2009, The potential for water savings through the control of saltcedar and Russian olive: Saltcedar and Russian olive control demonstration act science assessment. Scientific Investigations Report, v. 5247, p. 35-47.

Naranjo, J. B., Weiler, M., and Stahl, K., 2011, Sensitivity of a data-driven soil water balance model to estimate summer evapotranspiration along a forest chronosequence: Hydrology and Earth System Sciences, v. 15, no. 11, p. 3461.

Perignon, M. C., Tucker, G. E., Griffin, E. R., and Friedman, J. M., 2013, Effects of riparian vegetation on topographic change during a large flood event, Rio Puerco, New Mexico, USA: Journal of Geophysical Research: Earth Surface, v. 118, no. 3, p. 1193-1209.

Runyan, C., and Welty, C., 2010, Use of the White Method to estimate evapotranspiration along an urban riparian corridor: CUERE Technical Report 2010/001. UMBC, Center for Urban Environmental ….

Simpson, S. C., Meixner, T., and Hogan, J. F., 2013, The role of flood size and duration on streamflow and riparian groundwater composition in a semi-arid basin: Journal of Hydrology, v. 488, p. 126-135.

TxSON, 2019, Texas Soil Observation Network (TxSON), Bureau of Economic Geology, The University of Texas at Austin, http://coastal.beg.utexas.edu/soilmoisture/#/, accessed July 30, 2019.

Unland, N., Cartwright, I., Rau, G., Reed, J., Gilfedder, B., Atkinson, A., and Hofmann, H., 2013, Investigating the spatio-temporal variability in groundwater and surface water interactions: a multi-technique approach: Hydrology and Earth System Sciences, v. 17, no. 9, p. 3437.

Van Rossum, G., and Drake, F. L., 2011, The python language reference manual, Network Theory Ltd.

Vincent, K. R., Friedman, J. M., and Griffin, E. R., 2009, Erosional Consequence of Saltcedar Control: Environmental Management, v. 44, no. 2, p. 218-227.

Wang, T.-Y., Yu, J.-J., Wang, P., Min, L.-L., Pozdniakov, S. P., and Yuan, G.-F., 2019, Estimating groundwater evapotranspiration by phreatophytes using combined water level and soil moisture observations: Ecohydrology, v. 12, no. 5, p. e2092.

White, W. N., 1932, A method of estimating ground-water supplies based on discharge by plants and evaporation from soil: Results of investigations in Escalante Valley, Utah. U.S. Geological Survey Water-Supply Paper 659.

Wilcox, B. P., 2002, Shrub control and streamflow on rangelands: a process based viewpoint: Rangeland Ecology & Management/Journal of Range Management Archives, v. 55, no. 4, p. 318-326.

Wilcox, B. P., Owens, M. K., Dugas, W. A., Ueckert, D. N., and Hart, C. R., 2006, Shrubs, streamflow, and the paradox of scale: Hydrological Processes, v. 20, no. 15, p. 3245-3259.

Winter, T. C., Harvey, J. W., Franke, O. L., and Alley, W. M., 1998, Ground water and surface water: A single resource. U.S. Geological Survey Circular 1139.

Yu, M., Cartwright, I., Braden, J., and De Bree, S., 2013, Examining the spatial and temporal variation of groundwater inflows to a valley-to-floodplain river using 222 Rn, geochemistry and river discharge: the Ovens River, southeast Australia: Hydrology and Earth System Sciences, v. 17, no. 12, p. 4907-4924.